Bioorganic & Medicinal Chemistry xxx (2014) xxx–xxx

Contents lists available at ScienceDirect

Bioorganic & Medicinal Chemistry

journal homepage: www.elsevier.com/locate/bmc

Design and discovery of 5-hydroxy-6-oxo-1, 6-dihydropyrimidine-4-carboxamide inhibitors of HIV-1 integrase

Daoguang Zhang [a,†], Bikash Debnath [b,†], Shenghui Yu [a], Tino Wilson Sanchez [c], Frauke Christ [d], Yang Liu [a], Zeger Debyser [d], Nouri Neamati [b,*], Guisen Zhao [a,*]

[a] Department of Medicinal Chemistry, Key Laboratory of Chemical Biology (Ministry of Education), School of Pharmaceutical Sciences, Shandong University, Jinan, Shangdong 250012, China
[b] Department of Medicinal Chemistry, College of Pharmacy, University of Michigan, Ann Arbor, MI 48109, USA
[c] Department of Pharmacology and Pharmaceutical Sciences, School of Pharmacy, University of Southern California, Los Angeles, CA 90089, USA
[d] Laboratory for Molecular Virology and Gene Therapy, Division of Molecular Medicine, KU Leuven (KULeuven), Kapucijnenvoer 33, B-3000 Leuven, Flanders, Belgium

ARTICLE INFO

Article history:
Received 17 May 2014
Revised 20 July 2014
Accepted 22 July 2014
Available online xxxx

Keywords:
HIV-1 integrase inhibitors
INSTIs
5-Hydroxy-6-oxo-1,6-dihydropyrimidine analogues

ABSTRACT

Raltegravir (RAL) is a first clinically approved integrase (IN) inhibitor for the treatment of HIV but rapid mutation of the virus has led to chemo-resistant strains. Therefore, there is a medical need to develop new IN inhibitors to overcome drug resistance. At present, several IN inhibitors are in different phases of clinical trials and few have been discontinued due to toxicity and lack of efficacy. The development of potent second-generation IN inhibitors with improved safety profiles is key for selecting new clinical candidates. In this article, we report the design and synthesis of potent 5-hydroxy-6-oxo-1,6-dihydropyrimidine-4-carboxamide analogues as second-generation IN inhibitors. These compounds satisfy two structural requirements known for potent inhibition of HIV-1 IN catalysis: a metal chelating moiety and a hydrophobic functionality necessary for selectivity against the strand transfer reaction. Most of the new compounds described herein are potent and selective for the strand transfer reaction and show antiviral activity in cell-based assays. Furthermore, this class of compounds are drug-like and suitable for further optimization and preclinical studies.

1. Introduction

Reverse transcriptase, integrase (IN), and protease are the only viral enzymes responsible for HIV-replication. IN plays a pivotal role in the integration of the viral genome into the host genome enabling HIV to efficiently propagate in human $CD4^+$ cells. Because of the lack of a cellular homologue and its essential role in viral replication, IN remains a promising target for antiretroviral-based therapy.[1–3] Many efforts have been made to develop antiretroviral drugs targeting IN and Raltegravir (RAL) was the first FDA approved IN inhibitor.[4,5] Currently, more than thirty drugs have been approved for treating HIV infection targeting alternate stages.[6,7] Unfortunately, continuous mutation of the viral genome leads to multi-drug resistant viral strains that are no longer susceptible to current therapy including RAL.[8–10] Therefore, development of second-generation inhibitors have been the norm since the discovery of the first approved drug, AZT, nearly 30 years ago.[11] Currently, two other IN inhibitors (Elvitegravir and Dolutegravir) have been approved for clinical use and several other inhibitors targeting IN catalysis are in clinical trials.[12] Efforts are ongoing to develop allosteric inhibitors targeting IN dimerization and LEDGF/p75-IN interaction.[13–17]

HIV-1 IN is a 32 kDa polynucleotidyl transferase comprising three domains: the N-terminal domain, the C-terminal domain, and the catalytic domain. The catalytic domain contains a DDE motif (D64, D116, and E152) that forms metal chelating interactions with one or two divalent metal ions, such as Mn^{2+} and Mg^{2+}. IN catalyzes the insertion of reverse transcribed viral DNA into the host cell's chromosomes in two steps: (a) 3′-processing, the excision of two terminal nucleotides leaving 3′-hydroxyl ends of the viral DNA, and (b) strand transfer, insertion of the 3′-hydroxyl ends onto the host DNA by a nucleophilic addition.[18–20]

Abbreviations: CPE, cytopathic effect; LEDGF/p75, lens epithelium-derived growth factor; DMAD, dimethylacetylenedicarboxylate; IN, integrase; PK, pharmacokinetics; PD, pharmacodynamics; RAL, raltegravir; ELV, elvitegravir.

* Corresponding authors. Tel.: +1 734 647 2732; fax: +1 734 763 8152 (N.N.); tel./fax: +86 531 8838 2009 (G.Z.).
E-mail addresses: neamati@med.umich.edu (N. Neamati), guisenzhao@sdu.edu.cn (G. Zhao).
† These authors contributed equally.

http://dx.doi.org/10.1016/j.bmc.2014.07.036
0968-0896/

Over the past decade, extensive efforts were made to develop IN inhibitors with diverse chemical features, such as oligonucleotides, peptides, hydroxylated aromatics, hydrazides, quinoline derivatives, and quinolones.[21–29] In many cases the development of these inhibitors stalled due to undesired pharmacokinetics and/or toxicity. In addition to the success of RAL, several IN strand transfer inhibitors (INSTIs) are in different stages of clinical development (Fig. 1). Elvitegravir (ELV) and Dolutegravir were approved by the US FDA more recently and MK-2048 is in Phase II clinical trials, while MK-0536 and PICA are in pre-clinical stages.[30,31]

Cross-resistance of INSTIs has also been observed. For example, clinical isolates and recombinant molecular clones selected by RAL showed similar resistance to ELV. For instance, an E92Q/N155H IN double mutant selected by RAL and ELV reduces inhibition efficacy between 100–300 fold. Subsequent secondary mutations further diminish inhibitory activity while second-generation inhibitors are showing improved efficacy against RAL and ELV mutagenic pathways.[32–34] Taken together, new second-generation INSTIs with metal chelating groups and substituted phenyl rings such as the compounds discussed here are needed to further investigate the structure-activity relationships amongst this promising class of IN inhibitors.

2. Results and discussion

Previously, Summa et al. reported on the synthesis, optimization, and PK properties of a series of 4,5-dihydroxypyrimidine carboxamides and *N*-alkyl-5-hydroxypyrimidinone carboxamides.[35,36] On the basis of these reports, other studies leading to the development of RAL[5] and a number of other IN inhibitors in different stages of clinical development, we designed a series of 5-hydroxy-6-oxo-1,6-dihydropyrimide-4-carboxamide analogues including metal chelating groups and substituted phenyl rings.

2.1. Chemistry

The general synthetic route to target compounds **6** is depicted in Scheme l. The raw materials **1** were obtained from commercial sources (TCI, Tokyo kasei kogyo co., ltd). The key intermediates, amidoximes **2**, were synthesized from the corresponding nitrile **1** with hydroxylamine hydrochloride and potassium carbonate in an alcoholic solution. The synthesis of the key core methyl 5-hydroxy-6-oxo-1,6-dihydropyrimidine-4-carboxylate was achieved by conversion of the amidoximes **2** with DMAD into intermediate **3**, followed by cyclization with xylene at reflux affording the desired intermediate **4**. Finally, the compounds from the **6** series were synthesized by the ammonolysis reaction of methyl ester **4** with substituted benzylamine (**5**) as the nucleophilic reagent in a DMF solution.

2.2. Inhibition of HIV-1 integrase

The inhibition of HIV-1 IN catalytic activity was determined as previously described.[37] The **6** series of compounds that had *para* halogen substitutions in the phenyl ring of the carboxamide side showed potent activity and selectivity for strand transfer reaction (**6-a1**, IC_{50} = 0.6 μM; **6-a2**, IC_{50} = 0.8 μM, **6-a3**, IC_{50} = 0.5 μM). The presence of a phenyl halogen flanking metal chelating groups has been identified as an important component of several INSTIs in clinical trials. However, **6–a5** had methyl groups and still retained potency (IC_{50} = 0.5 μM) suggesting the scaffold can also tolerate alternate groups (Table 1).

The remaining compounds screened in this series were less potent IN inhibitors. Lengthening the distance between the carboxamide and the phenyl moiety with an additional carbon decreased potency against strand transfer seven-fold (**6-a7**, IC_{50} = 4 μM) while 3′-processing was unaffected. When the fluorine was changed to the 2 or 3 position of the phenyl, the inhibitory activity decreased depending on the position. Substitution of the phenyl halogen with a hydroxy or methoxy group also affected strand transfer inhibition (**6-a6**, IC_{50} = 2 μM; **6-a9**, IC_{50} = 6 μM) while non-substituted phenyl rings (**6-b1**) led to an eight-fold reduction in inhibition compared to the *para*-fluorinated analogue.

The **6** series of compounds followed a similar pattern of activity as RAL and other INSTIs in clinical trials. The overall scaffold of these compounds had the two basic moieties indicative of the INSTI class, a metal-chelating group flanked by a fluorinated phenyl. The distance between the fluorine and the nearest metal chelating member in all of the INSTIs in clinical trials remained at seven atoms that helps explaining the altered activity observed in compounds with halogens in the 2 or 3 position of phenyl ring. The scaffold also included a third ring opposite of the fluorinated phenyl linking the carboxamide. The addition of a methylene linker between the phenyl and pyrimidine ring (**6-c1**), opposite of the carboxamide, resulted in nearly a 20-fold reduction in strand transfer inhibition (IC_{50} = 10 μM).

The in vitro data suggest that the pyrimidines in this series displayed selectivity for the strand transfer reaction. Like other INSTIs, the more active compounds had a halogen in the *para* position,

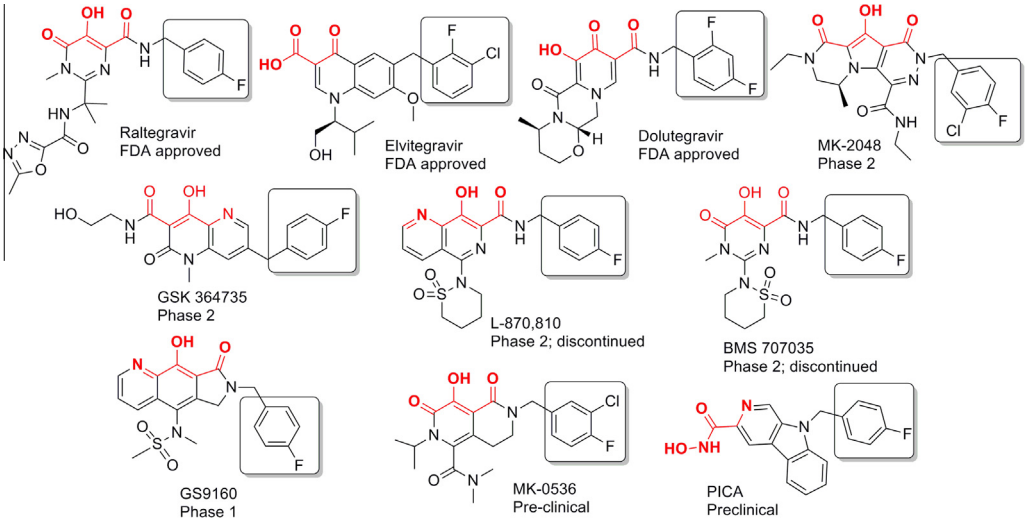

Figure 1. IN inhibitors in different stages of clinical development.

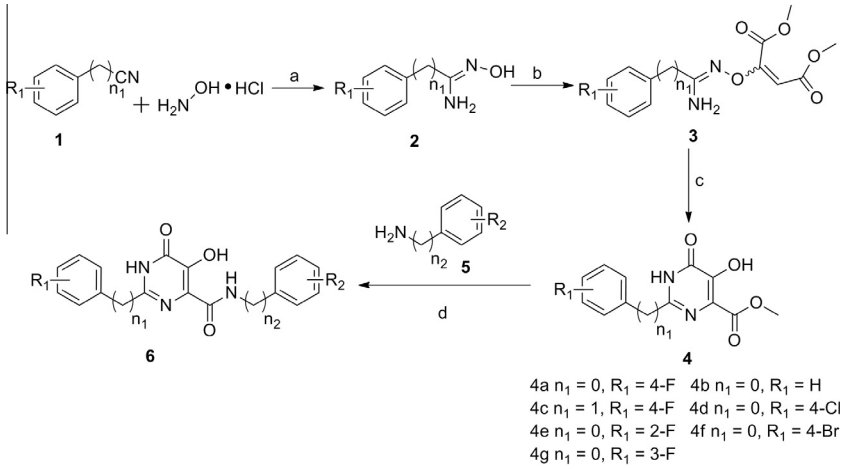

Scheme 1. Reagents and conditions: (a) K_2CO_3, C_2H_5OH, room temp, 30 min, then reflux for 12 h; (b) DMAD, anhyd CH_3OH, room temp for 12 h; (c) xylene, room temp for 2 h, 90 °C for 2 h, then reflux for 24 h; (d) anhyd DMF, reflux for 14 h.

Table 1
Inhibition of HIV-1 integrase catalytic activities by select 5-hydroxy-6-oxo-1,6-dihydropyrimidine-4-carboxamides

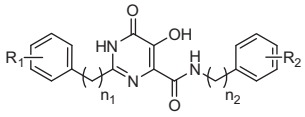

Code	n_1	n_2	R_1	R_2	Inhibition of HIV-1 IN (IC_{50} μM)	
					3′-Processing	Strand transfer
6-a1	0	1	4-F	4-F	12 ± 6	0.6 ± 0.2
6-a2	0	1	4-F	4-Cl	9 ± 7	0.8 ± 0.2
6-a3	0	1	4-F	4-Br	11 ± 6	0.5 ± 0.1
6-a4	0	1	4-F	3,4-F	17 ± 5	1 ± 0.4
6-a5	0	1	4-F	3,4-CH_3	16 ± 6	0.5 ± 0.04
6-a6	0	1	4-F	4-OCH_3	16 ± 6	2 ± 0.3
6-a7	0	2	4-F	4-F	17 ± 5	4 ± 1
6-a8	0	1	4-F	3-Cl	20	1.4 ± 0.9
6-a9	0	1	4-F	4-OH	>20	6 ± 3
6-a10	0	1	4-F	3-F	20 ± 1	3 ± 0.1
6-a11	0	1	4-F	2-F	20	7 ± 4
6-a12	0	1	4-F	2-F-3-Cl	13 ± 2	1.4 ± 0.1
6-a13	0	1	4-F	4-F-3-Cl	6 ± 4	4 ± 2
6-a14	0	1	4-F	3,4,5-F	14 ± 8	8 ± 0.1
6-b1	0	1	H	H	>20	8 ± 5
6-b2	0	1	H	4-F	17	1 ± 0.1
6-c1	1	1	4-F	4-F	>20	10 ± 2
6-d1	0	1	4-Cl	4-F	5	2 ± 0.4
6-e1	0	1	2-F	4-F	16 ± 6	2 ± 0.1
6-f1	0	1	4-Br	4-F	3	1 ± 0.1
6-g1	0	1	3-F	4-F	5	1

although a dimethylated phenyl displayed a comparable inhibitory profile. This similarity in activity observed with the dimethylated compound and the difluorinated analogue suggests this compound should be explored further.

2.3. Lead compounds show antiviral activity in cell-based assays

To assess whether the inhibition of the in vitro enzymatic activities can be translated into phenotypic activity, compounds were screened during HIV IIIB infection in MT-4 lymphocytes. The inhibitory effect of these compounds on the HIV-1-induced cytopathic effect (CPE) was determined by the MTT assay.[38] Table 2 lists antiviral and cytotoxic activities of select compounds. Compound **6-a1** inhibited HIV-1 replication with an EC_{50} value of 1.72 μM and showed a 26 fold therapeutic advantage compared to its cytotoxicity profile in MT-4 cells (therapeutic index, TI). Although the in vitro activities of the *para*-halogenated compounds were equally potent, the antiviral profile of the compounds with chlorine and bromine in the *para* position had a significant decrease in inhibition and thus a less favorable TI.

The dimethylated compound, **6-a5**, had a slightly improved antiviral inhibitory profile compared with a diflourinated analogue, a pattern also observed against IN catalysis in vitro. Although altering the 3-fluorine to chlorine of the difluorinated analogue reduced inhibition in vitro, **6-a13** had the best antiviral activity and the greatest therapeutic index (EC_{50} = 1.3 μM and CC_{50} = 45.5 μM). Another compound **6-a8** had a chlorine in the 3 position and showed significant inhibition of HIV-1 replication with minimal cytotoxicity in MT-4 cells, while the fluorinated analogue did not exhibit the same potency in vivo. Altering the distance between the carboxamide carbonyl and the fluorinated phenyl with an additional carbon (**6-a7**) failed to show anti-HIV activity at 30 μM, reinforcing the notion that a fixed distance between the metal chelating moiety and the phenyl fluorine is essential for improved inhibition (Table 2).

Table 2
Antiviral activities of 5-hydroxy-6-oxo-1,6-dihydropyrimidine-4-carboxamides

Compound	Activity in MT-4 cells		
	HIV-1 EC_{50} (μM)[a]	Cytotoxicity CC_{50} (μM)[b]	TI[c]
6-b1	5.65 ± 1.19	50.7 ± 7	9
6-a1	1.72 ± 1.22	44 ± 15	26
6-a2	8.1 ± 2.2	44 ± 3	5
6-a3	11.03 ± 0.73	47.5 ± 1.5	4
6-a4	5.17 ± 0.45	31 ± 9	6
6-a5	2.7 ± 0.29	33.5 ± 10.5	12
6-a6	7.61 ± 0.07	44 ± 5	6
6-a7	>30	30	
6-a8	1.91 ± 0.25	35 ± 9	18
6-a9	6.71 ± 0.73	49 ± 5	7
6-a10	7.34 ± 0.49	49.5 ± 1.5	7
6-a11	7.81 ± 2.34	28.5 ± 4.5	4
6-a12	2.61 ± 0.27	48 ± 0	18
6-a13	1.3	45.5 ± 1.5	35
6-a14	4.64 ± 1.76	34.5 ± 9.5	7

[a] Effective concentration required to reduce HIV-1-induced cytopathic effect by 50% in MT-4 cells.
[b] Cytotoxic concentration to reduce MT-4 cell viability by 50%.
[c] Therapeutic index: ratio CC_{50}/EC_{50}.

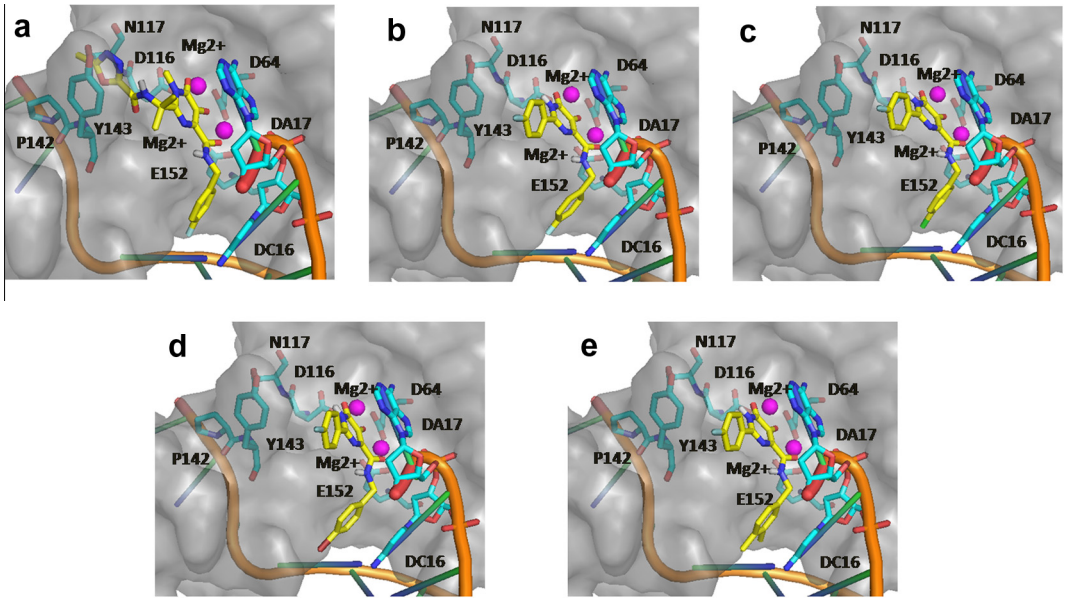

Figure 2. Binding poses for IN inhibitors (yellow colored). Inhibitors form metal chelation with Mg^{2+} (pink) along with key IN residues (cyan). (a) RAL; (b) **6-a1**; (c) **6-a2**; (d) **6-a3**; (e) **6-a5**.

2.4. Molecular docking study

Compounds **6-a1**, **6-a2**, **6-a3**, and **6-a5** were docked on the active site of IN to better understand their binding properties (Fig. 2). The docking pose of RAL reveals a similar binding mechanism with the exception of an aromatic ring absent in the **6** series that comes in close contact with IN Y143, an important residue in another mutagenic pathway resistant to RAL.[39] The two carbonyl oxygens and the hydroxylate ion of the dihydropyrimidine-4-carboxamide moiety of these active compounds function to chelate with two Mg^{2+} ions along with IN residues D64, D116, and E152. The docking pose shows the dihydropyrimidine ring can form pi–pi interactions with the viral nucleotide DA17. These docking results also suggest the phenyl ring attached to the carboxamide can form pi–pi stacking interactions with the viral nucleotide DC16. Thus, the binding mechanism of these compounds likely displaces the reactive DNA 3′OH from the metal chelation site and blocks the intasome activity.

3. Conclusion

The present study focuses on the design and synthesis of catalytic IN inhibitors based on RAL as well as other agents in clinical trials. Basic structural frameworks of these designed compounds include metal chelating groups and substituted phenyl rings likely forming interactions with the IN active site residues and viral DNA nucleotides. As expected, these 5-hydroxy-6-oxo-1,6-dihydropyrimidine-4-carboxamide analogs showed significant inhibition and strand transfer selectivity by chelation of metal ions perhaps by binding to key IN residues (D64, D116, and E152) at the catalytic binding site. Molecular docking suggests the binding mechanism could evade the Y143R/C mutagenic pathway that is observed after long exposure to RAL. Analogues from this series of INSTIs show antiviral activity without significant cytotoxicity in HIV-1 infected cells. Further preclinical PK/PD studies as well as lead optimization are warranted to select clinically viable compound for development.

4. Experimental section

4.1. Chemistry

Unless otherwise noted, all materials were obtained from commercial suppliers and used without further purification. All melting points were determined in a Büchi capillary melting point apparatus and are uncorrected. The proton nuclear magnetic resonance (^{1}H NMR) spectra were recorded with a Bruker Avance DRX600 instrument with tetramethyl-silane (TMS) as the internal standard. The chemical shifts (δ) were reported in parts per million (ppm) and were relative to the central peak of DMSO-d_6. Coupling constants (J) are given in Hz. and reported as follow: chemical shift, multiplicity (s = singlet, d = doublet, t = triplet, br = broad, m = multiplet), coupling constants, and number of protons. The ^{13}C NMR spectra were recorded with a Bruker Avance DRX400 instrument. The chemical shifts (δ) are reported in ppm relative to the centerline of the septet at 40.0 ppm for DMSO-d_6. The high-resolution mass spectra data were obtained using an Accela UPLC-LTQ Orbitrap Mass Spectrometer. Column chromatography was carried out with silica gel in the solvents indicated. Thin-layer chromatography (TLC) was performed on silica gel GF254 plates (layer thickness, 0.2 mm) and compounds were visualized using UV light. Petroleum ether used for TLC and column chromatography had a boiling range of 60–90 °C. All tested compounds showed more than 95% purity on the basis of HPLC analysis. The specific method for HPLC analysis and a table of the data for all tested compounds are presented in the Supporting information.

4.1.1. Synthesis of the compound 2 series

Hydroxylamine hydrochloride (200 mmol) and K_2CO_3 (200 mmol) were dissolved in 200 mL of alcohol and stirred for 30 min at room temperature. The corresponding nitriles (75 mmol) **1** were added and the reaction mixture was heated to reflux for 12 h. After filtration of inorganic salts, the solvent was evaporated under reduced pressure. The products **2** were purified by column chromatography (petroleum ether/acetone, 2:1, v/v).

4.1.1.1. 4-Fluoro-*N*-hydroxybenzimidamide (2a). White powder, yield 66.5%, mp: 79.4–80.1 °C. ^{1}H NMR (DMSO-d_6) δ (ppm): 9.66 (s, 1H), 7.71 (m, 2H), 7.20 (m, 2H), 5.84 (s, 2H).

4.1.1.2. *N*-Hydroxybenzimidamide (2b). White powder, yield 65.8%, mp: 72.1–73.2 °C. ^{1}H NMR (DMSO-d_6) δ (ppm): 9.62 (s, 1H), 7.67(m, 2H), 7.36 (m, 3H), 5.80 (s, 2H).

4.1.1.3. 2-(4-Fluorophenyl)-*N*-hydroxyacetimidamide (2c). White powder, yield 69.7%, mp: 79.3–81.2 °C. ^{1}H NMR (DMSO-d_6) δ (ppm): 8.89 (s, 1H), 7.30(m, 2H), 7.10 (m, 2H), 5.41 (s, 2H), 3.24 (s, 2H).

4.1.1.4. 4-Chloro-*N*-hydroxybenzimidamide (2d). White powder, yield 71.6%, mp: 124.3–126.4 °C. ^{1}H NMR (DMSO-d_6) δ (ppm): 9.73 (s, 1H), 7.69 (dd, J = 6.6 Hz, J = 2.4 Hz, 2H), 7.44 (dd, J = 6.6 Hz, J = 1.8 Hz, 2H), 5.87 (s, 2H).

4.1.1.5. 2-Fluoro-*N*-hydroxybenzimidamide (2e). Yellowish oil, yield 65.4%. ^{1}H NMR (DMSO-d_6) δ (ppm): 9.64 (s, 1H), 7.50 (t, J = 7.2 Hz, 1H), 7.43 (m, 1H), 7.24 (m, 2H), 5.82 (s, 2H).

4.1.1.6. 4-Bromo-*N*-hydroxybenzimidamide (2f). White powder, yield 67.8%, mp: 142.9–144.5 °C. ^{1}H NMR (DMSO-d_6) δ (ppm): 9.74 (s, 1H), 7.62 (dt, J = 8.4 Hz, J = 2.4 Hz, 2H), 7.57 (dt, J = 9.0 Hz, J = 2.4 Hz, 2H), 5.87 (s, 2H).

4.1.1.7. 3-Fluoro-*N*-hydroxybenzimidamide (2g). Yellowish powder, yield 67.3%, mp: 70.1–71.8 °C. ^{1}H NMR (DMSO-d_6) δ (ppm): 9.80 (s, 1H), 7.55 (d, J = 8.4 Hz, 1H), 7.47 (dt, J = 9.6 Hz, J = 1.2 Hz, 1H), 7.42 (m, 1H), 7.21 (td, J = 8.4 Hz, J = 2.4 Hz, 1H), 5.91 (s, 2H).

4.1.2. Synthesis of the compound 3 series

Compounds in series **2** (20 mmol) were dissolved in 50 mL of distilled methanol under anhydrous conditions. 1.2 equiv of dimethylacetylenedicarboxylate (24 mmol) was added drop-wise with external cooling. The reaction mixture was stirred for 14 h at room temperature and then concentrated under vacuum. Brown oil (**3**) was obtained, which was used for the next step without further purification.

4.1.3. Synthesis of the compound 4 series

An amount of 20 mmol of compounds **3** were dissolved in 100 mL of xylene, obtaining a brown solution. The brown solution was stirred at room temperature for 2 h, 90 °C for 2 h, and then refluxed for 24 h under a nitrogen atmosphere. The reaction mixture was stirred at room temperature for 2 h to allow the precipitation of the product as a light-brown solid. The resulting solid was collected by filtration and then was washed with ether to afford compounds **4**.

4.1.3.1. Methyl 2-(4-fluorophenyl)-5-hydroxy-6-oxo-1,6-dihydropyrimidine-4-carboxylate (4a). Yellowish powder, yield 38.6%, mp: 262.3–264.1 °C. ^{1}H NMR (DMSO-d_6) δ (ppm): 13.11 (br, 1H), 10.54 (br, 1H), 8.07 (dd, J = 7.8 Hz, J = 6.0 Hz, 2H), 7.35 (t, J = 8.4 Hz, 2H), 3.85 (s, 3H).

4.1.3.2. Methyl 5-hydroxy-6-oxo-2-phenyl-1,6-dihydropyrimidine-4-carboxylate (4b). Pink powder, yield 46.4%, mp: 243.4–245.1 °C. ^{1}H NMR (DMSO-d_6) δ (ppm): 13.11 (br, 1H), 10.52 (br, 1H), 8.06 (d, J = 6.0 Hz, 2H), 7.53 (m, 3H), 3.88 (s, 3H).

4.1.3.3. Methyl 2-(4-fluorobenzyl)-5-hydroxy-6-oxo-1,6-dihydropyrimidine-4-carboxylate (4c). Gray powder, yield 41.3%, mp: 261.3–263.4 °C. ^{1}H NMR (DMSO-d_6) δ (ppm): 12.95 (br, 1H), 10.28 (br, 1H), 7.32 (dd, J = 7.8 Hz, J = 6.0 Hz, 2H), 7.15 (t, J = 9.0 Hz, 2H), 3.82 (s, 3H), 3.80 (s, 2H).

4.1.3.4. Methyl 2-(4-chlorophenyl)-5-hydroxy-6-oxo-1,6-dihydropyrimidine-4-carboxylate (4d). Pink powder, yield 43.2%, mp: 271.7–273.6 °C. ^{1}H NMR (DMSO-d_6) δ (ppm): 13.17 (br, 1H), 10.58 (br, 1H), 8.03 (d, J = 8.4 Hz, 2H), 7.58 (dt, J = 9.0 Hz, J = 2.4 Hz, 2H), 3.86 (s, 3H).

4.1.3.5. Methyl 2-(2-fluorophenyl)-5-hydroxy-6-oxo-1,6-dihydropyrimidine-4-carboxylate (4e). Yellowish powder, yield 39.7%, mp: 235.1–236.7 °C. 13.14 (br, 1H), 10.63 (br, 1H), 7.65 (t, J = 7.8 Hz, 1H), 7.59 (m, 1H), 7.35 (m, 2H), 3.83 (s, 3H).

4.1.3.6. Methyl 2-(4-bromophenyl)-5-hydroxy-6-oxo-1,6-dihydropyrimidine-4-carboxylate (4f). Yellowish powder, yield 44.5%, mp: 260.6–261.9 °C. ^{1}H NMR (DMSO-d_6) δ (ppm): 13.18 (br, 1H), 10.61 (br, 1H), 7.95 (d, J = 9.0 Hz, 2H), 7.72 (d, J = 8.4 Hz, 2H), 3.85 (s, 3H).

4.1.3.7. Methyl 2-(3-fluorophenyl)-5-hydroxy-6-oxo-1,6-dihydropyrimidine-4-carboxylate (4g). Yellowish powder, yield 39.7%, mp: 262.3–264.1 °C. ^{1}H NMR (DMSO-d_6) δ (ppm): 13.19 (br, 1H), 10.64 (br, 1H), 7.88 (d, J = 7.8 Hz, 1H), 7.83 (d, J = 10.8 Hz, 1H), 7.56 (m, 1H), 7.38 (td, J = 8.4 Hz, J = 2.4 Hz, 1H), 3.88 (s, 3H).

4.1.4. Synthesis of the compounds in the 6 series

To a stirred solution of compounds **4** (5 mmol) in *N*,*N*-dimethylformamide (20 mL), substituted benzylamine (3 equiv) was added and the resulting mixture was stirred at 90 °C for 12 h under a nitrogen atmosphere. After the mixture was cooled at room temperature, distilled water (150 mL) and 1 N HCl (15 mL) was added. The resulting solid was collected by filtration and then was re-crystallized from *N*,*N*-dimethylformamide/water to afford compounds **6**.

4.1.4.1. *N*-(4-Fluorobenzyl)-2-(4-fluorophenyl)-5-hydroxy-6-oxo-1,6-dihydropyrimidine-4-carboxamide (6-a1). White powder, yield 94.2%, mp: 262.8–264.6 °C. ^{1}H NMR (DMSO-d$_6$) δ (ppm): 12.96 (br, 1H), 12.55 (br, 1H), 9.65 (s, 1H), 8.33 (dd, J = 9.0 Hz, J = 6.0 Hz, 2H), 7.40 (dd, J = 9.0 Hz, J = 6.0 Hz, 2H), 7.35 (t, J = 9.0 Hz, 2H), 7.17 (t, J = 9.0 Hz, 2H), 4.52 (d, J = 6.6 Hz, 2H). ^{13}C NMR (100 MHz, DMSO-d_6) δ (ppm): 42.00, 115.47, 115.68, 115.77, 115.99, 127.38, 128.75, 129.84, 129.92, 130.51, 130.60, 135.30, 135.33, 145.66, 148.41, 158.92, 160.55, 162.96, 163.01, 165.48, 169.16. HRMS (ESI) m/z calcd for $C_{18}H_{14}F_2N_3O_3$ [M+H]$^+$: 358.0998, found 358.1000.

4.1.4.2. *N*-(4-Chlorobenzyl)-2-(4-fluorophenyl)-5-hydroxy-6-oxo-1,6-dihydropyrimidine-4-carboxamide (6-a2). Yellowish powder, yield 92.6%, mp: 273.8–274.9 °C. ^{1}H NMR (DMSO-d_6) δ (ppm): 12.96 (br, 1H), 12.52 (br, 1H), 9.67 (t, J = 6.6 Hz, 1H), 8.34 (dd, J = 9.0 Hz, J = 6.0 Hz, 2H), 7.38 (m, 6H), 4.53 (d, J = 6.6 Hz, 2H). ^{13}C NMR (100 MHz, DMSO-d_6) δ (ppm): 42.10, 115.75, 115.97, 127.50, 128.79, 129.71, 129.81, 130.51, 130.60, 132.07, 138.14, 145.84, 148.31, 158.96, 163.01, 165.48, 169.22. HRMS (ESI) m/z calcd for $C_{18}H_{14}ClFN_3O_3$ [M+H]$^+$: 374.0702, found 374.0709.

4.1.4.3. *N*-(4-Bromobenzyl)-2-(4-fluorophenyl)-5-hydroxy-6-oxo-1,6-dihydropyrimidine-4-carboxamide (6-a3). Yellowish powder, yield 90.3%, mp: 269.4–271.5 °C. ^{1}H NMR (DMSO-d_6) δ (ppm): 12.98 (br, 1H), 12.51 (br, 1H), 9.67 (s, 1H), 8.32 (dd, J = 7.8 Hz, J = 5.4 Hz, 2H), 7.54 (d, J = 9.0 Hz, 2H), 7.34 (m, 4H), 4.51 (d, J = 6.6 Hz, 2H). ^{13}C NMR (100 MHz, DMSO-d_6) δ (ppm): 42.15, 115.77, 115.98, 120.52, 127.38, 128.74, 130.07, 130.52,

130.60, 131.71, 138.57, 145.71, 148.39, 158.92, 163.01, 165.49, 169.22. HRMS (ESI) *m/z* calcd for $C_{18}H_{14}BrFN_3O_3$ $[M+H]^+$: 418.0197, found 418.0201.

4.1.4.4. *N*-(3,4-Difluorobenzyl)-2-(4-fluorophenyl)-5-hydroxy-6-oxo-1,6-dihydropyrimidine-4-carboxamide (6-a4). Yellowish powder, yield 93.3%, mp: 278.2–279.6 °C. ^{1}H NMR (DMSO-d_6) δ (ppm): 12.98 (br, 1H), 12.43 (br, 1H), 9.60 (s, 1H), 8.33 (dd, J = 8.4 Hz, J = 6.0 Hz, 2H), 7.45 (dd, J = 15.0 Hz, J = 8.4 Hz, 1H), 7.36 (t, J = 9.0 Hz, 2H), 7.25 (td, J = 8.4 Hz, J = 2.4 Hz, 1H), 7.09 (td, J = 8.4 Hz, J = 2.4 Hz, 1H), 4.56 (d, J = 6.0 Hz, 2H). ^{13}C NMR (100 MHz, DMSO-d_6) δ (ppm): 36.06, 36.10, 103.90, 104.16, 104.41, 111.78, 111.82, 111.99, 112.03, 115.77, 115.99, 122.00, 122.04, 122.15, 122.19, 127.31, 128.69, 130.52, 130.60, 131.14, 131.20, 131.24, 131.30, 145.72, 148.38, 158.91, 159.05, 159.18, 160.64, 160.76, 161.51, 161.64, 163.01, 163.08, 163.20, 165.49, 169.29. HRMS (ESI) *m/z* calcd for $C_{18}H_{13}F_3N_3O_3$ $[M+H]^+$: 376.0904, found 376.0906.

4.1.4.5. *N*-(3,4-Dimethylbenzyl)-2-(4-fluorophenyl)-5-hydroxy-6-oxo-1,6-dihydropyrimidine-4-carboxamide (6-a5). Yellowish powder, yield 94.1%, mp: 252.1–254.3 °C. ^{1}H NMR (DMSO-d_6) δ (ppm): 12.95 (br, 1H), 12.65 (br, 1H), 9.58 (s, 1H), 8.33 (dd, J = 8.4 Hz, J = 5.4 Hz, 2H), 7.34 (t, J = 9.0 Hz, 2H), 7.08 (m, 3H), 4.45 (d, J = 6.6 Hz, 2H), 2.20 (s, 3H), 2.18 (s, 3H). ^{13}C NMR (100 MHz, DMSO-d_6) δ (ppm): 19.45, 19.84, 42.47, 115.75, 115.97, 125.33, 127.61, 128.81, 129.07, 129.89, 130.52, 130.61, 135.26, 136.38, 136.46, 145.71, 148.36, 158.97, 163.00, 165.47, 169.03. HRMS (ESI) *m/z* calcd for $C_{20}H_{19}FN_3O_3$ $[M+H]^+$: 368.1405, found 368.1408.

4.1.4.6. *N*-(4-Methoxybenzyl)-2-(4-fluorophenyl)-5-hydroxy-6-oxo-1,6-dihydropyrimidine-4-carboxamide (6-a6). Brown powder, yield 93.2%, mp: 244.6–246.3 °C. ^{1}H NMR (DMSO-d_6) δ (ppm): 12.95 (br, 1H), 12.65 (br, 1H), 9.58 (s, 1H), 8.33 (dd, J = 7.8 Hz, J = 5.4 Hz, 2H), 7.35 (t, J = 9.0 Hz, 2H), 7.29 (d, J = 8.4 Hz, 2H), 6.90 (d, J = 8.4 Hz, 2H), 4.46 (d, J = 6.6 Hz, 2H), 3.73 (s, 3H). ^{13}C NMR (100 MHz, DMSO-d_6) δ (ppm): 42.15, 55.53, 114.25, 115.75, 115.97, 127.44, 128.73, 129.27, 130.51, 130.60, 131.06, 145.65, 148.45, 158.87, 163.00, 165.48, 169.01. HRMS (ESI) *m/z* calcd for $C_{19}H_{17}FN_3O_4$ $[M+H]^+$: 370.1198, found 370.1199.

4.1.4.7. *N*-(4-Fluorophenethyl)-2-(4-fluorophenyl)-5-hydroxy-6-oxo-1,6-dihydropyrimidine-4-carboxamide (6-a7). Yellowish powder, yield 89.7%, mp: 239.5–241.3 °C. ^{1}H NMR (DMSO-d_6) δ (ppm): 12.94 (br, 1H), 12.65 (br, 1H), 9.11 (s, 1H), 8.29 (dd, J = 9.0 Hz, J = 5.4 Hz, 2H), 7.36 (t, J = 9.0 Hz, 2H), 7.31 (dd, J = 9.0 Hz, J = 5.4 Hz, 2H), 7.14 (t, J = 9.0 Hz, 2H), 3.55 (dd, J = 15.0 Hz, J = 6.0 Hz, 2H), 2.90 (t, J = 7.2 Hz, 2H). ^{13}C NMR (100 MHz, DMSO-d_6) δ (ppm): 34.45, 40.73, 115.48, 115.69, 115.76, 115.98, 127.40, 128.79, 130.44, 130.53, 130.83, 130.91, 135.56, 135.59, 145.67, 148.21, 158.94, 160.19, 162.60, 163.01, 165.48, 168.91. HRMS (ESI) *m/z* calcd for $C_{19}H_{16}F_2N_3O_3$ $[M+H]^+$: 372.1154, found 372.1156.

4.1.4.8. *N*-(3-Chlorobenzyl)-2-(4-fluorophenyl)-5-hydroxy-6-oxo-1,6-dihydropyrimidine-4-carboxamide (6-a8). Yellowish powder, yield 90.9%, mp: 296.2–297.3 °C. ^{1}H NMR (DMSO-d_6) δ (ppm): 12.97 (br, 1H), 12.46 (br, 1H), 9.67 (s, 1H), 8.33 (dd, J = 8.4 Hz, J = 5.4 Hz, 2H), 7.37 (m, 6H), 4.54 (d, J = 6.6 Hz, 2H). ^{13}C NMR (100 MHz, DMSO-d_6) δ (ppm): 42.20, 115.78, 116.00, 126.55, 127.46, 127.66, 128.72, 130.51, 130.60, 130.77, 133.47, 141.70, 145.69, 148.42, 158.95, 163.01, 165.49, 169.26. HRMS (ESI) *m/z* calcd for $C_{18}H_{14}ClFN_3O_3$ $[M+H]^+$: 374.0702, found 374.0705.

4.1.4.9. *N*-(4-Hydroxybenzyl)-2-(4-fluorophenyl)-5-hydroxy-6-oxo-1,6-dihydropyrimidine-4-carboxamide (6-a9). Brown powder, yield 92.4%, mp: 281.3–282.7 °C. ^{1}H NMR (DMSO-d_6) δ (ppm): 12.95 (br, 1H), 12.70 (br, 1H), 9.54 (s, 1H), 9.33 (s, 1H), 8.32 (dd, J = 8.4 Hz, J = 5.4 Hz, 2H), 7.34 (t, J = 9.0 Hz, 2H), 7.17 (d, J = 8.4 Hz, 2H), 6.72 (d, J = 9.0 Hz, 2H), 4.42 (d, J = 6.0 Hz, 2H). ^{13}C NMR (100 MHz, DMSO-d_6) δ (ppm): 42.23, 115.57, 115.75, 115.96, 127.43, 128.72, 129.26, 130.52, 130.61, 145.62, 148.44, 156.93, 158.90, 162.76, 163.00, 165.47, 168.93. HRMS (ESI) *m/z* calcd for $C_{18}H_{15}FN_3O_4$ $[M+H]^+$: 356.1041, found 356.1044.

4.1.4.10. *N*-(3-Fluorobenzyl)-2-(4-fluorophenyl)-5-hydroxy-6-oxo-1,6-dihydropyrimidine-4-carboxamide (6-a10). Yellowish powder, yield 93.3%, mp: 286.1–288.1 °C. ^{1}H NMR (DMSO-d_6) δ (ppm): 12.92 (br, 1H), 12.51 (br, 1H), 9.68 (s, 1H), 8.34 (dd, J = 9.0 Hz, J = 6.0 Hz, 2H), 7.26 (dd, J = 13.8 Hz, J = 7.2 Hz, 1H), 7.35 (t, J = 8.4 Hz, 2H), 7.19 (m, 2H), 7.10 (m, 1H), 4.55 (d, J = 6.0 Hz, 2H). ^{13}C NMR (100 MHz, DMSO-d_6) δ (ppm): 42.23, 114.15, 114.36, 114.41,114.62, 115.78,115.99, 123.77, 123.80, 127.49, 128.80, 130.51, 130.60, 130.78, 130.86, 142.04, 142.11, 145.74, 148.36, 158.99, 161.46, 163.01, 163.88, 165.48, 169.27. HRMS (ESI) *m/z* calcd for $C_{18}H_{14}F_2N_3O_3$ $[M+H]^+$: 358.0998, found 358.1001.

4.1.4.11. *N*-(2-Fluorobenzyl)-2-(4-fluorophenyl)-5-hydroxy-6-oxo-1,6-dihydropyrimidine-4-carboxamide (6-a11). Yellowish powder, yield 92.6%, mp: 264.3–265.7 °C. ^{1}H NMR (DMSO-d_6) δ (ppm): 12.98 (br, 1H), 12.47 (br, 1H), 9.61 (s, 1H), 8.34 (dd, J = 8.4 Hz, J = 6.0 Hz, 2H), 7.35 (m, 4H), 7.20 (m, 2H), 7.19 (m, 2H), 4.59 (d, J = 6.6 Hz, 2H). ^{13}C NMR (100 MHz, DMSO-d_6) δ (ppm): 36.44, 36.49, 115.50, 115.71, 115.77, 115.98, 124.87, 124.91, 125.62, 125.76, 127.38, 128.72, 129.48, 129.56, 129.79, 129.84, 130.53, 130.62, 145.72, 148.38, 158.90, 159.16, 161.59, 163.02, 165.49, 169.30. HRMS (ESI) *m/z* calcd for $C_{18}H_{14}F_2N_3O_3$ $[M+H]^+$: 358.0998, found 358.1001.

4.1.4.12. *N*-(3-Chloro-2-fluorobenzyl)-2-(4-fluorophenyl)-5-hydroxy-6-oxo-1,6-dihydropyrimidine-4-carboxamide (6-a12). Brown powder, yield 87.9%, mp: 289.3–291.8 °C. ^{1}H NMR (DMSO-d_6) δ (ppm): 12.99 (br, 1H), 12.38 (br, 1H), 9.65 (s, 1H), 8.33 (m, 2H), 7.52 (d, J = 7.2 Hz, 1H), 7.36 (m, 3H), 7.22 (t, J = 8.4 Hz, 1H), 4.62 (d, J = 6.6 Hz, 2H). ^{13}C NMR (100 MHz, DMSO-d_6) δ (ppm): 36.58, 36.63, 115.76, 115.98, 119.91, 120.09, 125.75, 125.80, 127.31, 127.79, 127.93, 128.77, 128.81, 129.79, 130.53, 130.61, 145.79, 148.37, 154.30, 156.76, 158.90, 163.03, 165.50, 169.35. HRMS (ESI) *m/z* calcd for $C_{18}H_{13}ClF_2N_3O_3$ $[M+H]^+$: 392.0608, found 392.0612.

4.1.4.13. *N*-(3-Chloro-4-fluorobenzyl)-2-(4-fluorophenyl)-5-hydroxy-6-oxo-1,6-dihydropyrimidine-4-carboxamide (6-a13). Yellowish powder, yield 90.8%, mp: 270.9–272.7 °C. ^{1}H NMR (DMSO-d_6) δ (ppm): 12.98 (br, 1H), 12.44 (br, 1H), 9.66 (s, 1H), 8.33 (m, 2H), 7.57 (d, J = 6.6 Hz, 1H), 7.38 (m, 4H), 4.52 (d, J = 6.6 Hz, 2H). HRMS (ESI) *m/z* calcd for $C_{18}H_{13}ClF_2N_3O_3$ $[M+H]^+$: 392.0608, found 392.0612.

4.1.4.14. *N*-(3,4,5-Trifluorobenzyl)-2-(4-fluorophenyl)-5-hydroxy-6-oxo-1,6-dihydropyrimidine-4-carboxamide (6-a14). Yellowish powder, yield 90.3%, mp: 268.7–270.9 °C. ^{1}H NMR (DMSO-d_6) δ (ppm): 12.99 (br, 1H), 12.35 (br, 1H), 9.65 (s, 1H), 8.33 (dd, J = 7.8 Hz, J = 5.4 Hz, 2H), 7.36 (t, J = 9.0 Hz, 2H), 7.31 (t, J = 7.8 Hz, 2H), 4.52 (d, J = 6.6 Hz, 2H). HRMS (ESI) *m/z* calcd for $C_{18}H_{12}F_4N_3O_3$ $[M+H]^+$: 394.0809, found 394.0814.

4.1.4.15. *N*-Benzyl-5-hydroxy-6-oxo-2-phenyl-1,6-dihydropyrimidine-4-carboxamide (6-b1). White powder, yield 94.5%, mp: 251.4–252.5 °C. ^{1}H NMR (DMSO-d_6) δ (ppm): 12.95

(br, 1H), 12.61 (br, 1H), 9.63 (s, 1H), 8.25 (d, J = 7.2 Hz, 2H), 7.51 (m, 3H), 7.35 (m, 4H), 7.27 (m, 1H), 4.54 (d, J = 6.0 Hz, 2H). HRMS (ESI) m/z calcd for $C_{18}H_{16}N_3O_3$ $[M+H]^+$: 322.1186, found 322.1191.

4.1.4.16. *N*-(4-Fluorobenzyl)-5-hydroxy-6-oxo-2-phenyl-1, 6-dihydropyrimidine-4-carboxamide (6-b2). White powder, yield 92.6%, mp: 248.7–250.3 °C. ^{1}H NMR (DMSO-d_6) δ (ppm): 12.94 (br, 1H), 12.56 (br, 1H), 9.62 (t, J = 6.0 Hz, 1H), 8.25 (d, J = 7.8 Hz, 2H), 7.52 (m, 3H), 7.40 (dd, J = 8.4 Hz, J = 6.0 Hz, 2H), 7.17 (m, 2H), 4.52 (d, J = 6.0 Hz, 2H). HRMS (ESI) m/z calcd for $C_{18}H_{15}FN_3O_3$ $[M+H]^+$: 340.1092, found 340.1098.

4.1.4.17. *N*,2-Bis(4-fluorobenzyl)-5-hydroxy-6-oxo-1,6-dihydropyrimidine-4-carboxamide (6-c1). White powder, yield 87.2%, mp: 220.5–222.2 °C. ^{1}H NMR (DMSO-d_6) δ (ppm): 12.84 (br, 1H), 12.35 (br, 1H), 9.37 (t, J = 6.0 Hz, 1H), 7.39 (m, 4H), 7.16 (m, 4H), 4.46 (d, J = 6.0 Hz, 2H), 3.81 (s, 2H). HRMS (ESI) m/z calcd for $C_{19}H_{16}F_2N_3O_3$ $[M+H]^+$: 372.1154, found 372.1160.

4.1.4.18. *N*-(4-Fluorobenzyl)-2-(4-chlorophenyl)-5-hydroxy-6-oxo-1,6-dihydropyrimidine-4-carboxamide (6-d1). White powder, yield 89.9%, mp: 290.7–292.2 °C. ^{1}H NMR (DMSO-d_6) δ (ppm): 13.00 (br, 1H), 12.61 (br, 1H), 9.67 (s, 1H), 8.29 (d, J = 8.4 Hz, 2H), 7.58 (d, J = 8.4 Hz, 2H), 7.40 (dd, J = 9.0 Hz, J = 6.0 Hz, 2H), 7.17 (t, J = 9.0 Hz, 2H), 4.52 (d, J = 6.6 Hz, 2H). HRMS (ESI) m/z calcd for $C_{18}H_{14}ClFN_3O_3$ $[M+H]^+$: 374.0702, found 374.0709.

4.1.4.19. *N*-(4-Fluorobenzyl)-2-(2-fluorophenyl)-5-hydroxy-6-oxo-1,6-dihydropyrimidine-4-carboxamide (6-e1). White powder, yield 93.4%, mp: 214.8–216.1 °C. ^{1}H NMR (DMSO-d_6) δ (ppm): 12.95 (br, 1H), 12.63 (br, 1H), 9.46 (t, J = 6.0 Hz, 1H), 7.81 (t, J = 7.2 Hz, 1H), 7.59 (dd, J = 13.8 Hz, J = 6.0 Hz, 1H), 7.36 (m, 4H), 7.16 (t, J = 9.0 Hz, 2H), 4.46 (d, J = 7.8 Hz, 2H). HRMS (ESI) m/z calcd for $C_{18}H_{14}F_2N_3O_3$ $[M+H]^+$: 358.0998, found 358.1003.

4.1.4.20. *N*-(4-Fluorobenzyl)-2-(4-bromophenyl)-5-hydroxy-6-oxo-1,6-dihydropyrimidine-4-carboxamide (6-f1). White powder, yield 90.6%, mp: 295.6–297.2 °C. ^{1}H NMR (DMSO-d_6) δ (ppm): 13.00 (br, 1H), 12.61 (br, 1H), 9.66 (s, 1H), 8.21 (d, J = 8.4 Hz, 2H), 7.71 (d, J = 8.4 Hz, 2H), 7.40 (dd, J = 8.4 Hz, J = 6.0 Hz, 2H), 7.17 (t, J = 9.0 Hz, 2H), 4.52 (d, J = 6.0 Hz, 2H). HRMS (ESI) m/z calcd for $C_{18}H_{14}BrFN_3O_3$ $[M+H]^+$: 418.0197, found 418.0203.

4.1.4.21. *N*-(4-Fluorobenzyl)-2-(3-fluorophenyl)-5-hydroxy-6-oxo-1,6-dihydropyrimidine-4-carboxamide (6-g1). White powder, yield 90.6%, mp: 277.3–279.4 °C. ^{1}H NMR (DMSO-d_6) δ (ppm): 13.01 (br, 1H), 12.65 (br, 1H), 9.70 (s, 1H), 8.22 (d, J = 10.8 Hz, 1H), 8.10 (d, J = 7.8 Hz, 1H), 7.55 (dd, J = 15.0 Hz, J = 7.2 Hz, 1H), 7.39 (m, 3H), 7.18 (t, J = 9.0 Hz, 2H), 4.53 (d, J = 6.6 Hz, 2H). HRMS (ESI) m/z calcd for $C_{18}H_{14}F_2N_3O_3$ $[M+H]^+$: 358.0998, found 358.1004.

4.2. Biological materials, chemicals and enzymes

All compounds were dissolved in DMSO and the 10 mM stock solutions were stored at −20 °C. Further dilutions were also performed in DMSO. The expression system used in purifying IN was a kind gift from Dr. Robert Craigie, Laboratory of Molecular Biology, NIDDK, NIH, Bethesda, MD. The oligonucleotides used in the HIV-1 IN catalytic activity assay were synthesized at the USC Norris Cancer Center microsequencing core facility. The γ [^{32}P]-ATP was purchased from Perkin-Elmer (Waltham, MA).

4.3. Preparation of oligonucleotide substrate

The HIV-1 IN catalytic activity assay uses a 21′mer top strand: (5′-GTGTGGAAAATCTCTAGCAGT-3′), and a 21′mer bottom strand: (5′-ACTGCTAGAGATTTTCCACAC-3′). The top strand was labeled at the 5′end with γ [^{32}P]-ATP by T4 polynucleotide kinase (Epicenter, Madison, WI). The mixture was then incubated at 95 °C for 15 min to inactivate the kinase and the bottom strand was added in 1.5 molar excess. The strands were allowed to anneal by cooling the mixture slowly to room temperature. Any unincorporated material was subsequently removed by centrifuging the mixture through a Spin-25 mini-column (USA Scientific, Ocala, FL).

4.4. Integrase catalytic activity assay

The extent of 3′-processing and strand transfer was analyzed by pre-incubating recombinant wild-type HIV-1 IN, at a final concentration of 200 nM, with the inhibitor in reaction buffer (50 mM NaCl, 1 mM HEPES, pH 7.5, 50 μM EDTA, 50 μM dithiothreitol, 10% glycerol (w/v), 7.5 mM MnCl2, 0.1 mg/mL bovine serum albumin, 10 mM 2-mercaptoethanol, 10% DMSO, and 25 mM MOPS, pH 7.2) at 30 °C for 30 min. Then 20 nM of the ^{32}P 5′end-labeled linear 21′mer substrate was added, and incubation was continued for an additional 1 h. Reactions were then quenched by the addition of an equal volume (16 μL) of loading dye (98% deionized formamide, 10 mM EDTA, 0.025% xylene cyanol, and 0.025% bromophenol blue). An aliquot (7 μL) was electrophoresed on a denaturing 20% polyacrylamide gel (0.09 M tris–borate pH 8.3, 2 mM EDTA, 20% acrylamide, 8 M urea). Gels were dried, exposed in a PhosphorImager cassette, analyzed using a Typhoon 8610 Variable Mode Imager (Amersham Biosciences), and quantified using ImageQuant 5.2. The percent inhibition (%I) was calculated using the following equation:%I = 100*[1−(D − C)/(N − C)] where C, N, and D are the fractions of 21-mer substrate converted to 19-mer (3′-processing product) or strand transfer products for DNA alone, DNA plus IN, and IN plus drug, respectively. The IC_{50} values were determined by plotting the logarithm of drug concentration against percent inhibition of enzymatic activity to obtain the concentration that produced 50% inhibition.

4.5. In vitro anti-HIV and drug susceptibility assays

The inhibitory effect of antiviral drugs on the HIV-1-induced CPE in human lymphocyte MT-4 cell culture was determined by the MTT assay.[38] This assay is based on the reduction of the yellow colored 3-(4,5-dimethylthiazol-2-yl)-2,5-diphenyltetrazolium bromide (MTT) by mitochondrial dehydrogenase of metabolically active cells to a blue formazan derivative, which can be measured spectrophotometrically. The 50% cell culture infective dose ($CCID_{50}$) of the HIV-1 (IIIB) strain was determined by titration of the virus stock using MT-4 cells. For the drug susceptibility assays, MT-4 cells were infected with 100–300 $CCID_{50}$ of the virus stock in the presence of 5-fold serial dilutions of the antiviral drugs. The concentration of various compounds achieving 50% protection against the CPE of the HIV strain, which is defined as the EC_{50}, was determined. In parallel, the 50% cytotoxic concentration (CC_{50}) was determined.

4.6. Molecular docking

Molecular docking studies were performed using GOLD (genetic optimization for ligand docking) software package, version 4.0 (Cambridge Crystallographic Data Centre, Cambridge, U.K.) in the catalytic binding site of a homology model of HIV-1 integrase reported earlier.[37] GOLD uses a genetic algorithm to explore the conformational space of a compound inside the binding site of a protein.[40,41] The active site was defined as the collection of protein

residues with a sphere of 15 Å radius. Before docking different possible stereomers, ionized forms and conformations of ligands are prepared by LigPrep (Schrodinger, LLC). Ionization option, epik was used to ionize ligands at pH 7.0 ± 0.2.[42,43] Docking studies were performed using the standard default settings with 100 genetic algorithm (GA) runs on each molecule. For each of the 100 independent GA runs, a maximum of 100,000 operations were performed on a set of 5 groups with a population of 100 individuals. With respect to ligand flexibility special care has been taken by including options such as flipping of ring corners, amides, pyramidal nitrogens, secondary and tertiary amines, and rotation of carboxylate groups, as well as torsion angle distribution and post-process rotatable bonds as default. The annealing parameters were used as default cutoff values of 3.0 Å for H-bonds and 4.0 Å for van der Waals interactions. Hydrophobic fitting points were calculated to facilitate the correct starting orientation of the compound for docking by placing the hydrophobic atoms appropriately in the corresponding areas of the active site. When the top three solutions attained root-mean-square deviation (rmsd) values within 1.5 Å, docking was terminated. GOLD-Score, a scoring function within the software, is a dimensionless fitness value that takes into account the intra- and intermolecular H-bonding interaction energy, van der Waals energy, and ligand torsion energy.[40,41]

Acknowledgments

The work in GZ laboratory was supported by a grant from the National Natural Science Foundation of China (Grant Numbers: 20872082 and 21272140). The work in NN and ZD laboratories were supported by funds from an NIH/NIAID (R21 AI081610) grant. TWS was funded by the NIH F31 (AI082942-01) and CHRP (D08-USC-321) awards.

Supplementary data

Supplementary data associated with this article can be found, in the online version, at http://dx.doi.org/10.1016/j.bmc.2014.07.036.

References and notes

1. Quashie, P. K.; Sloan, R. D.; Wainberg, M. A. *BMC Med.* **2012**, *10*, 34.
2. Neamati, N. *HIV-1 Integrase: Mechanism and Inhibitor Design*; Wiley, 2011.
3. Asante-Appiah, E.; Skalka, A. M. *Antiviral Res.* **1997**, *36*, 139.
4. Egbertson, M.; Anthony, N. J.; Vincenzo Summa, V. *HIV Integrase Inhibitors: From Diketoacids to Heterocyclic Templates: A History of HIV Integrase Medicinal Chemistry at Merck West Point and Merck Rome (IRBM) Leading to the Discovery of Raltegravir*; Wiley, 2011.
5. Summa, V.; Petrocchi, A.; Bonelli, F.; Crescenzi, B.; Donghi, M.; Ferrara, M.; Fiore, F.; Gardelli, C.; Gonzalez Paz, O.; Hazuda, D. J.; Jones, P.; Kinzel, O.; Laufer, R.; Monteagudo, E.; Muraglia, E.; Nizi, E.; Orvieto, F.; Pace, P.; Pescatore, G.; Scarpelli, R.; Stillmock, K.; Witmer, M. V.; Rowley, M. *J. Med. Chem.* **2008**, *51*, 5843.
6. Zeier, M. D.; Nachega, J. B. *Infect. Disord. Drug Targets* **2011**, *11*, 98.
7. Mehellou, Y.; De Clercq, E. *J. Med. Chem.* **2010**, *53*, 521.
8. Malet, I.; Delelis, O.; Soulie, C.; Wirden, M.; Tchertanov, L.; Mottaz, P.; Peytavin, G.; Katlama, C.; Mouscadet, J. F.; Calvez, V.; Marcelin, A. G. *J. Antimicrob. Chemother.* **2009**, *63*, 795.
9. Wirden, M.; Simon, A.; Schneider, L.; Tubiana, R.; Malet, I.; Ait-Mohand, H.; Peytavin, G.; Katlama, C.; Calvez, V.; Marcelin, A. G. *J. Antimicrob. Chemother.* **2009**, *64*, 1087.
10. Ramkumar, K.; Neamati, N. *Core Evid.* **2010**, *4*, 131.
11. Pendri, A.; Meanwell, N. A.; Peese, K. M.; Walker, M. A. *Expert Opin. Ther. Pat.* **2011**, *21*, 1173.
12. McColl, D. J.; Chen, X. *Antiviral Res.* **2010**, *85*, 101.
13. Demeulemeester, J.; Tintori, C.; Botta, M.; Debyser, Z.; Christ, F. *J. Biomol. Screen.* **2012**, *17*, 618.
14. Christ, F.; Shaw, S.; Demeulemeester, J.; Desimmie, B. A.; Marchand, A.; Butler, S.; Smets, W.; Chaltin, P.; Westby, M.; Debyser, Z.; Pickford, C. *Antimicrob. Agents Chemother.* **2012**.
15. De Luca, L.; Ferro, S.; Morreale, F.; Christ, F.; Debyser, Z.; Chimirri, A.; Gitto, R. *J. Enzyme Inhib. Med. Chem.* **2012**.
16. Peat, T. S.; Rhodes, D. I.; Vandegraaff, N.; Le, G.; Smith, J. A.; Clark, L. J.; Jones, E. D.; Coates, J. A.; Thienthong, N.; Newman, J.; Dolezal, O.; Mulder, R.; Ryan, J. H.; Savage, G. P.; Francis, C. L.; Deadman, J. J. *PLoS ONE* **2012**, *7*, e40147.
17. Al-Mawsawi, L. Q.; Neamati, N. *ChemMedChem* **2011**, *6*, 228.
18. Bacchi, A.; Carcelli, M.; Compari, C.; Fisicaro, E.; Pala, N.; Rispoli, G.; Rogolino, D.; Sanchez, T. W.; Sechi, M.; Sinisi, V.; Neamati, N. *J. Med. Chem.* **2011**, *54*, 8407.
19. Long, Y. Q.; Jiang, X. H.; Dayam, R.; Sanchez, T.; Shoemaker, R.; Sei, S.; Neamati, N. *J. Med. Chem.* **2004**, *47*, 2561.
20. Kulkosky, J.; Jones, K. S.; Katz, R. A.; Mack, J. P.; Skalka, A. M. *Mol. Cell. Biol.* **1992**, *12*, 2331.
21. de Soultrait, V. R.; Desjobert, C.; Tarrago-Litvak, L. *Curr. Med. Chem.* **2003**, *10*, 1765.
22. Xu, Y. W.; Zhao, G. S.; Shin, C. G.; Zang, H. C.; Lee, C. K.; Lee, Y. S. *Bioorg. Med. Chem.* **2003**, *11*, 3589.
23. Krajewski, K.; Long, Y. Q.; Marchand, C.; Pommier, Y.; Roller, P. P. *Bioorg. Med. Chem. Lett.* **2003**, *13*, 3203.
24. Costi, R.; Santo, R. D.; Artico, M.; Massa, S.; Ragno, R.; Loddo, R.; La Colla, M.; Tramontano, E.; La Colla, P.; Pani, A. *Bioorg. Med. Chem.* **2004**, *12*, 199.
25. Benard, C.; Zouhiri, F.; Normand-Bayle, M.; Danet, M.; Desmaele, D.; Leh, H.; Mouscadet, J. F.; Mbemba, G.; Thomas, C. M.; Bonnenfant, S.; Le Bret, M.; d'Angelo, J. *Bioorg. Med. Chem. Lett.* **2004**, *14*, 2473.
26. Sato, M.; Motomura, T.; Aramaki, H.; Matsuda, T.; Yamashita, M.; Ito, Y.; Kawakami, H.; Matsuzaki, Y.; Watanabe, W.; Yamataka, K.; Ikeda, S.; Kodama, E.; Matsuoka, M.; Shinkai, H. *J. Med. Chem.* **2006**, *49*, 1506.
27. Snasel, J.; Rosenberg, I.; Paces, O.; Pichova, I. *J. Enzyme Inhib. Med. Chem.* **2009**, *24*, 241.
28. Wang, P.; Liu, C.; Sanches, T.; Zhong, Y.; Liu, B.; Xiong, J.; Neamati, N.; Zhao, G. *Bioorg. Med. Chem. Lett.* **2009**, *19*, 4574.
29. Korolev, S.; Knyazhanskaya, E.; Anisenko, A.; Tashlitskii, V.; Zatsepin, T. S.; Gottikh, M.; Agapkina, J. *Nucleosides, Nucleotides Nucleic Acids* **2011**, *30*, 651.
30. Johnson, B. C.; Metifiot, M.; Pommier, Y.; Hughes, S. H. *Antimicrob. Agents Chemother.* **2012**, *56*, 411.
31. Hare, S.; Vos, A. M.; Clayton, R. F.; Thuring, J. W.; Cummings, M. D.; Cherepanov, P. *Proc. Natl. Acad. Sci. U.S.A.* **2010**, *107*, 20057.
32. Van Wesenbeeck, L.; Rondelez, E.; Feyaerts, M.; Verheyen, A.; Van der Borght, K.; Smits, V.; Cleybergh, C.; De Wolf, H.; Van Baelen, K.; Stuyver, L. J. *Antimicrob. Agents Chemother.* **2011**, *55*, 321.
33. Shimura, K.; Kodama, E.; Sakagami, Y.; Matsuzaki, Y.; Watanabe, W.; Yamataka, K.; Watanabe, Y.; Ohata, Y.; Doi, S.; Sato, M.; Kano, M.; Ikeda, S.; Matsuoka, M. *J. Virol.* **2008**, *82*, 764.
34. Eshleman, S. H.; Hudelson, S. E.; Smith, P.; Hackett, J.; Holzmayer, V.; Swanson, P.; Devare, S. G.; Marlowe, N. *AIDS Res. Hum. Retroviruses* **2009**, *25*, 343.
35. Summa, V.; Petrocchi, A.; Matassa, V. G.; Gardelli, C.; Muraglia, E.; Rowley, M.; Paz, O. G.; Laufer, R.; Monteagudo, E.; Pace, P. *J. Med. Chem.* **2006**, *49*, 6646.
36. Pace, P.; Di Francesco, M. E.; Gardelli, C.; Harper, S.; Muraglia, E.; Nizi, E.; Orvieto, F.; Petrocchi, A.; Poma, M.; Rowley, M.; Scarpelli, R.; Laufer, R.; Gonzalez Paz, O.; Monteagudo, E.; Bonelli, F.; Hazuda, D.; Stillmock, K. A.; Summa, V. *J. Med. Chem.* **2007**, *50*, 2225.
37. Fan, X.; Zhang, F. H.; Al-Safi, R. I.; Zeng, L. F.; Shabaik, Y.; Debnath, B.; Sanchez, T. W.; Odde, S.; Neamati, N.; Long, Y. Q. *Bioorg. Med. Chem.* **2011**, *19*, 4935.
38. Pauwels, R.; Balzarini, J.; Baba, M.; Snoeck, R.; Schols, D.; Herdewijn, P.; Desmyter, J.; De Clercq, E. *J. Virol. Methods* **1988**, *20*, 309.
39. Delelis, O.; Thierry, S.; Subra, F.; Simon, F.; Malet, I.; Alloui, C.; Sayon, S.; Calvez, V.; Deprez, E.; Marcelin, A. G.; Tchertanov, L.; Mouscadet, J. F. *Antimicrob. Agents Chemother.* **2010**, *54*, 491.
40. Jones, G.; Willett, P.; Glen, R. C.; Leach, A. R.; Taylor, R. *J. Mol. Biol.* **1997**, *267*, 727.
41. Jones, G.; Willett, P. *Curr. Opin. Biotechnol.* **1995**, *6*, 652.
42. LigPrep, v., Schrödinger, LLC, New York, NY, 2011.
43. Epik, v., Schrödinger, LLC, New York, NY, 2011.